

# Antiferromagnetic resonances in twinned $\text{EuFe}_2\text{As}_2$ single crystal.

I. A. Golovchanskiy<sup>1,2</sup>, N.N. Abramov<sup>2</sup>, V.A. Vlasenko<sup>3</sup>, K. Pervakov<sup>3</sup>, I.V. Shchetinin<sup>2</sup>, P.S. Dzhumaev<sup>4</sup>, O.V. Emelianova<sup>4</sup>, D. Baranov<sup>1,4,5,6</sup>, V.M. Pudalov<sup>3,7</sup>, V.S. Stolyarov<sup>1,5</sup>

<sup>1</sup> *Moscow Institute of Physics and Technology, State University,  
9 Institutskiy per., Dolgoprudny, Moscow Region, 141700, Russia;*

<sup>2</sup> *National University of Science and Technology MISIS, 4 Leninsky prosp., Moscow, 119049, Russia;*

<sup>3</sup> *Ginzburg Center for High Temperature Superconductivity and Quantum Materials,  
P.N. Lebedev Physical Institute of the RAS, 119991, Moscow,*

*Russia;* <sup>4</sup> *National Research Nuclear University MEPhI (Moscow Engineering Physics Institute),  
31 Kashirskoye Shosse, 115409 Moscow, Russia;* <sup>5</sup> *Dukhov Research Institute of Automatics (VNIIA),  
127055 Moscow, Russia;* <sup>6</sup> *Skobeltsyn Institute of Nuclear Physics, MSU,  
Moscow, 119991, Russia;* <sup>7</sup> *HSE University, 101000 Moscow, Russia.*

In this work, we report ferromagnetic resonance spectroscopy of  $\text{EuFe}_2\text{As}_2$  single crystals. We observe ferromagnetic resonance responses, which are attributed to antiferromagnetic resonances of Eu sub-lattice with orthorhombic crystal structure and with different orientations of twin domains relative to the external field. We confirm validity of the recently-proposed spin Hamiltonian with anisotropic Eu-Eu exchange interaction and biquadratic Eu-Fe exchange interaction.

*Authors comment:* In the previous version of this manuscript (deposited on arXiv) we considered the helical spin order of Eu sub-lattice for explanation of the resonance spectrum. In layered magnetic systems, such as  $\text{EuFe}_2\text{As}_2$ , in absence of the in-plane easy axis the helical alignment is the only possible for explanation of resonances with negative-slope dependence of frequency on the magnetic field. However, in recently published works (Refs. [7,8]) it is demonstrated experimentally that the in-plane easy axis appears for Eu sub-lattice in layered  $\text{EuFe}_2\text{As}_2$  due to the biquadratic Eu-Fe exchange interaction and the spin-density wave antiferromagnetic order in the Fe sub-lattice. In this manuscript we report that the resonance spectrum of  $\text{EuFe}_2\text{As}_2$  can be well described qualitatively and quantitatively with the model proposed in Refs. [7,8].

## I. INTRODUCTION

For the last decade  $\text{EuFe}_2\text{As}_2$  compound has been of a high research interest [1–8]. As the major motivation,  $\text{EuFe}_2\text{As}_2$  is considered as a parent compound for the new class of ferromagnetic superconductors where superconducting and ferromagnetic spin ordering coexists on atomic scales of the crystal lattice. Superconductivity in  $\text{EuFe}_2\text{As}_2$ -based ferromagnetic superconductors emerges by doping it with phosphorus [9–14], or substituting europium layers with rubidium [15–21]. When it comes to the interplay between the superconductivity and the ferromagnetism, the studies are mainly focused on their superconducting properties and on the physical origin behind the emergence of superconductivity. In case of  $\text{EuFeAs}$ -based ferromagnetic superconductors the coexistence is considered between magnetic ordering of  $\text{Eu}^{2+}$  ions with large spin number  $S = 7/2$  and superconducting ordering of Fe-3d electrons.

However,  $\text{EuFe}_2\text{As}_2$  compound itself is rich in various magnetic phenomena. At about 190 K the crystal structure of  $\text{EuFe}_2\text{As}_2$  undergoes the tetragonal-to-orthorhombic phase transition [4, 7, 8] accompanied by the spin density wave antiferromagnetic transition in Fe sub-lattice. The direction of the spin density wave is locked along the longer  $a$  crystal axis of the orthorhombic structure (see Fig. 1). At about 20 K the Eu subsystem undergoes the A-type antiferromagnetic transition [5, 7, 8]. The orthorhombic crystal structure is naturally subjected to twinning, but also to magnetostriction

due to the movement of twin boundaries in response to changes of the magnetic field and magnetization of Eu sub-lattice [6–8]. The latter indicates Eu-Fe exchange interaction. This relocation of twin boundaries is one of the main obstructions for studies of magnetic ordering in  $\text{EuFe}_2\text{As}_2$  with magnetization measurements: upon magnetization the variation in fraction of differently oriented twin domains additionally impacts the magnetization. Only recently the complete microscopic form of magnetic interactions in  $\text{EuFe}_2\text{As}_2$  was established [7, 8]. It includes the anisotropic Eu-Eu exchange interaction, bi-quadratic Eu-Fe exchange interaction, and implies the spin-flip transition in A-type antiferromagnetic Eu sub-lattice when the magnetic field is applied along the  $a$  crystal axis. Metamagnetic transitions in  $\text{EuFe}_2\text{As}_2$  [3, 7, 8] are developed due to magnetization of twin domains with the  $\pi/2$  difference in their mutual orientation.

In this work, we consider magnetization dynamics in single crystal  $\text{EuFe}_2\text{As}_2$ . In general, ferromagnetic resonance (FMR) measurements are an ultimate tool for testing interlayer exchange interactions in various antiferromagnets [22–24]. In addition, FMR studies are free from the twinning problem, since the ratio of differently oriented twin domains impact the intensity but not the position of resonance lines. By observing and analysing antiferromagnetic resonance spectral lines we have found that the FMR spectrum confirms the validity of the 3D-expanded version of the spin Hamiltonian proposed in Ref. [8].

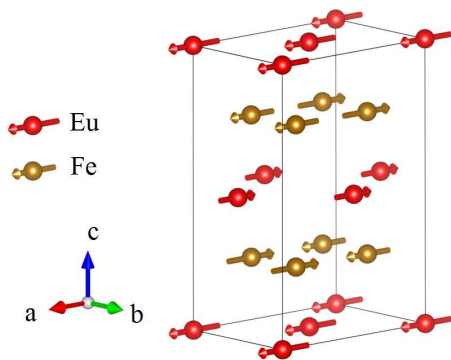


FIG. 1. Magnetic crystal structure of  $\text{EuFe}_2\text{As}_2$  (made using VESTA software). The crystal structure of  $\text{EuFe}_2\text{As}_2$  is orthorhombic with the space group  $Fmmm$  [4]. Fe spin sublattice is in spin density wave antiferromagnetic state aligned with the  $a$  axis. Eu spin sub-lattice is in A-type antiferromagnetic state.

## II. EXPERIMENTAL DETAILS

$\text{EuFe}_2\text{As}_2$  single crystals were grown using the self-flux method, by analogy with previous works [25, 26]. The initial high purity components of Eu (99.95%) and preliminary synthesized precursor FeAs (99.98% Fe+99.9999% As) were mixed with 1:6 molar ratio. The mixture was placed in an alumina crucible and sealed in a niobium tube under 0.2 atm of residual argon pressure. The sealed container was loaded into a tube furnace with an argon atmosphere to suppress the alkali metal evaporation. Next, the furnace was heated up to 1250°C, held at this temperature for 24 h to homogenize melting, and then cooled down to 900°C at a rate of 2°C/h. At this temperature, the ampoule with crystals was held for 24 h for growth defects elimination and then cooled down to room temperature inside the furnace. Finally, crystals were collected from the crucible in an argon glove box. Visually, as-synthesized bulk crystals demonstrate well-defined layered structure and their pliability for cleavage and exfoliation along the layering direction only. XRD studies confirm alignment of  $ab$  crystal planes within the layers, and orientation of  $c$  crystal axis across the layers. Samples for magnetization measurements and ferromagnetic resonance spectroscopy were obtained by cleavage of as-synthesized bulk crystals. Cleaved  $\text{EuFe}_2\text{As}_2$  samples were of a few mm in size along  $ab$  crystal planes, and about 50  $\mu\text{m}$  thick along the  $c$  crystal axis, which ensured the thin film geometry with defined crystal orientation.

Ferromagnetic resonance spectroscopy was performed using the VNA-FMR flip-chip approach [27, 28]. Cleaved  $\text{EuFe}_2\text{As}_2$  sample was glued on top of the transmission line of coplanar waveguide. The waveguide with impedance 50 Ohm and the width of the transmission line 0.5 mm is patterned on a Arlon AD1000 copper board and is equipped with SMP rf connectors. The board with the sample is installed in a brass sample holder. A

thermometer and a heater are attached directly to the holder for precise temperature control. The holder is placed in a home-made superconducting solenoid inside a closed-cycle cryostat (Oxford Instruments Triton, base temperature 1.2 K). Magnetic field is applied in-plane along the direction of the waveguide. The response of experimental samples is studied by analyzing the transmitted microwave signal  $S_{21}(f, H)$  with the VNA Rohde & Schwarz ZVB20.

## III. RESULTS AND DISCUSSIONS

Figure 2 shows FMR absorption spectra of  $\text{EuFe}_2\text{As}_2$  sample measured at magnetic field applied in-plane along  $ab$  layers at  $T = 5$  K and 20 K. At 5 K (Fig. 2a) the spectrum contains three absorption features (encircled with red dashed line): (i) a resonance line at  $0 < \mu_0 H \lesssim 0.5$  T and  $10 < f < 23$  GHz with a negative-slope linear field dependence, referred to as line I; (ii) a weaker resonance line at  $\mu_0 H \gtrsim 0.7$  T and  $18 < f < 22$  GHz, which also has approximately linear field dependence with a negative slope, referred to as line II; and (iii) an absorption “patch” at  $0.55 \lesssim \mu_0 H \lesssim 0.7$  T and  $f > 20$  GHz, referred to as the absorption feature III. A spectral line with the negative field-slope is commonly attributed to an antiferromagnetic resonance response.

At temperatures above 19 K (Figure 2b) the spectrum contains a single resonance line with the linear dependence of the resonance frequency on the magnetic field, corresponding to paramagnetic resonance of Eu spins. The field slope of the paramagnetic resonance  $f_r/2\pi\mu_0 H \approx 36.6$  GHz/T is slightly higher than the gyromagnetic ratio of free electrons 29 GHz/T indicating a possible contribution of residual susceptibility in the vicinity of the Curie temperature [29]. No dependence of the field slope on temperature was observed in the temperature range from 19 up to 30 K.

The spin configuration of Eu and Fe subsystems in  $\text{EuFe}_2\text{As}_2$  and the twinning problem were studied extensively in a number of previous works with neutron scattering and XMCD measurements. As a consensus [8], it is shown that at low temperature Fe sub-lattice is in the spin density wave antiferromagnetic state aligned with the longer side of orthorhombic lattice, while Eu sub-lattice has the A-type antiferromagnetic order (see Fig. 1). Importantly, Eu-Fe exchange interaction results in anisotropic Eu-Eu exchange interaction and in development of the easy axis along the direction of the spin density wave ( $a$ -direction) due to bi-quadratic Eu-Fe exchange. The total free energy of the spin configuration in a unit cell of Eu layers is [8]

$$F = 2(J + W)e_{1x}e_{2x} + 2(J - W)e_{1y}e_{2y} + 2Je_{1z}e_{2z} + 8K_a \sum_{i=1}^2 e_{ix}^2 + K_u \sum_{i=1}^2 e_{iz}^2 - M_s \sum_{i=1}^2 \vec{e}_i \vec{H}, \quad (1)$$

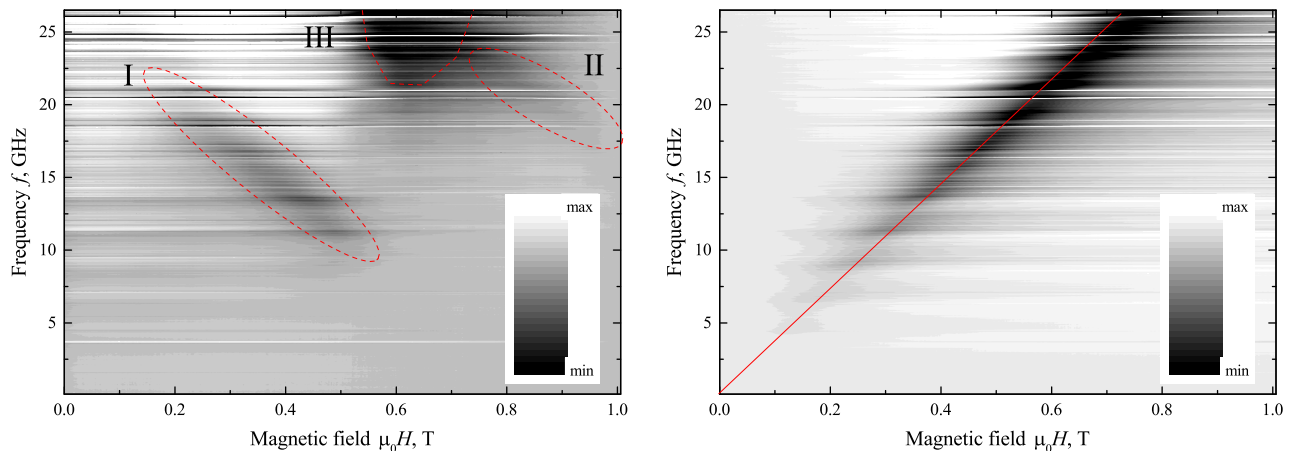


FIG. 2. FMR absorption spectra  $S_{21}(f, H)$  of  $\text{EuFe}_2\text{As}_2$  measured at  $T = 5$  K (a) and 20 K (b). Magnetic field is applied in-plane along  $ab$  crystal planes. Circular red dashed lines in (a) highlight three absorption features. Red line in (b) corresponds to the linear fit of the spectral line with the slope 36.6 GHz/T.

where  $e_{ix}$ ,  $e_{iy}$ , and  $e_{iz}$  are common components of the unit vector of magnetization orientation in spherical coordinates  $\vec{e} = \sin\theta \cos\phi \hat{x} + \sin\theta \sin\phi \hat{y} + \cos\theta \hat{z}$ ,  $[\hat{x}, \hat{y}, \hat{z}]$  axes are aligned with  $[a, b, c]$  crystal axes in Fig. 1, respectively, the first three terms are the exchange interaction terms, which are anisotropic in  $x$  and  $y$  directions by the parameter  $W$ , the fourth term is the bi-quadratic Eu-Fe exchange interaction in a form of the  $x$ -axis uniaxial anisotropy, the fifth term is the  $z$ -axis uniaxial anisotropy, and the last term is the Zeeman energy with the external field  $\vec{H}$ , which is applied in  $ab$  plane at the angle  $\phi_H$  with respect to the  $a$ -axis. In comparison to Ref. [8], two terms  $[2Je_{1z}e_{2z}]$  and  $[K_u \sum_{i=1}^2 e_{iz}^2]$  are added to complete the 3D representation of the free energy, and the Eu-Fe exchange interaction is redefined in the  $x$ -axis uniaxial form.

Following Ref. [8], exchange and anisotropy parameters of the free energy can be derived from the saturation fields. When magnetic field is applied along the  $b$  crystal axis, magnetization of Eu occurs via spin canting and the saturation field is  $H_b^{sat} = (4J + 16K_a)/M_s$ . When magnetic field is applied along the  $a$  crystal axis, magnetization occurs via spin-flip transition and the saturation field (i.e., the spin-flip field) is  $H_a^{sat} = 2(J + W)/M_s$ . When magnetic field is applied at  $45^\circ$  with respect to  $a$  or  $b$  direction, the saturation field is  $H_{45}^{sat} = 4J/M_s$ . The condition for the spin-flip transition is  $J/(8K_a + W) < 1$ . By expanding the treatment to the 3D case, the saturation field for field orientation along the  $c$  axis is  $H_c^{sat} = 2(J + K_u)/M_s$ .

The dependence of orientations of Eu magnetic moments on the magnetic field can be derived numerically by minimising the energy in Eq. 1 with predefined anisotropy and exchange parameters. By knowing orientations of Eu magnetic moments, ferromagnetic resonance of Eu can be derived using the Suhl-Smit-Beljers approach[30, 31] extended for the case of magnetization

dynamics in coupled magnetic multilayers [24, 32–34]. With this approach the following set of equations of motion for magnetization vector in each Eu layer defines the collective dispersion of the spin system with orientation along  $ab$  planes ( $\theta_i = \pi/2$ ):

$$i \frac{\omega M_s}{\gamma} \begin{bmatrix} \delta\theta_1 \\ \delta\theta_2 \\ \delta\phi_1 \\ \delta\phi_2 \end{bmatrix} = \begin{bmatrix} 0 & 0 & F_{\phi_1\phi_1} & F_{\phi_1\phi_2} \\ 0 & 0 & F_{\phi_1\phi_2} & F_{\phi_2\phi_2} \\ -F_{\theta_1\theta_1} & -F_{\theta_1\theta_2} & 0 & 0 \\ -F_{\theta_1\theta_2} & -F_{\theta_2\theta_2} & 0 & 0 \end{bmatrix} \begin{bmatrix} \delta\theta_1 \\ \delta\theta_2 \\ \delta\phi_1 \\ \delta\phi_2 \end{bmatrix}, \quad (2)$$

where  $\delta\theta_i$  and  $\delta\phi_i$  are components of small deviations of magnetization vector in spherical coordinates,  $F_{\theta_i\theta_j}$  and  $F_{\phi_i\phi_j}$  are corresponding second-order partial derivatives of the free energy (Eq. 1),  $\omega$  is the eigen-frequency of magnetization precession, and  $\gamma = 28$  GHz/T is the gyromagnetic ratio. The following expression  $\sum \cos(\phi_i - \phi_H) \delta\phi_i$  corresponds to the dynamic susceptibility of the resonance.

Figure 3 collects experimental and theoretical dependencies of FMR frequencies  $f_r$  on magnetic field. In calculations we consider the in-plane magnetic field aligned with  $ab$  crystal planes, with the angle  $\phi_H$  relative to the  $a$  crystal axis. In accordance with the twinning domain concept [6–8], the sample also contains domains where the orientation of the magnetic field is  $\pi/2 - \phi_H$  relative to the  $a$  crystal axis.

In general, our calculations showed that the value  $\phi_H$  is close to 0, which indicates that the sample consists of domains whose  $a$ -axis is aligned with the magnetic field and domains whose  $a$ -axis is perpendicular to the magnetic field. For the former domains at  $H < H_a^{sat}$  the spectrum consists of two antiferromagnetic spectral lines with linear-in-field increasing (decreasing) resonant frequency, attributed to individual resonances of oppositely-aligned Eu spin sub-lattices. At  $H > H_a^{sat}$  the spin flop transition occurs and the spectrum consist of two col-

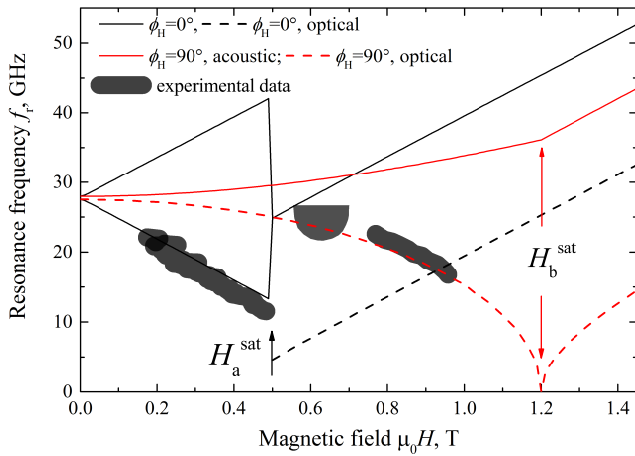


FIG. 3. Experimental and theoretical dependencies of the ferromagnetic resonance frequency on the magnetic field  $f_r(H)$ . Black lines show theoretical data for the domain with  $\phi_H = 0$ . Red lines show theoretical data for the domain with  $\phi_H = \pi/2$ . Solid lines show either individual resonances of Eu sublattices, as in case of  $\phi_H = 0$  and  $\mu_0 H < 0.5$ , or the collective acoustic response. Dashed lines show the collective optical response. Arrows indicate transition fields  $H_a^{sat}$  and  $H_b^{sat}$ .

lective modes: the higher-frequency acoustic mode and the lower-frequency optical mode, both with linear field dependence. Antiferromagnetic interaction between layers, which are magnetized to saturation, results in higher resonance frequency for the acoustic mode in comparison to the optical mode [34]. For the domains with the  $b$ -axis aligned with the magnetic field the spectrum also consists of two lines. At  $H < H_b^{sat}$  the spectrum contains collective modes: higher-frequency acoustic mode with positive frequency dependence on magnetic field, and the lower-frequency optical mode with negative frequency dependence on magnetic field. At  $H > H_b^{sat}$  the spin-flop transition (saturation) occurs manifested by a kink on both curves and both collective modes show positive dependence of frequency on magnetic field.

A rough numerical optimisation of magnetic parameters in Eqs.1 and 2 yields the following set of parameters, consistent with Ref. [8]:  $4J/M_s \approx 0.8$  T;  $2W/M_s \approx 0.2$  T;  $H_a^{sat} \approx 0.5$  T;  $H_b^{sat} = (4J + 16K_a)/M_s \approx 1.2$  T;  $2K_u/M_s \approx 0.25$  T;  $|\phi_H| < 5^\circ$ . According to Fig. 3, the spectral line I corresponds to the resonance of Eu spins aligned against the external field in the domain having the angle  $\phi_H = 0$  with the external field. The spectral line II corresponds to the optical antiferromagnetic response in the domain having the angle  $\phi_H = \pi/2$  with the external field. Its optical origin explains the low intensity in comparison with line I.

The spectral feature III in Figs. 2a and 3 may be attributed to the optical antiferromagnetic response in the same domain. In this case the change in the line intensity is a signature of the twin domain wall relocation when the fraction of these domains reduces with

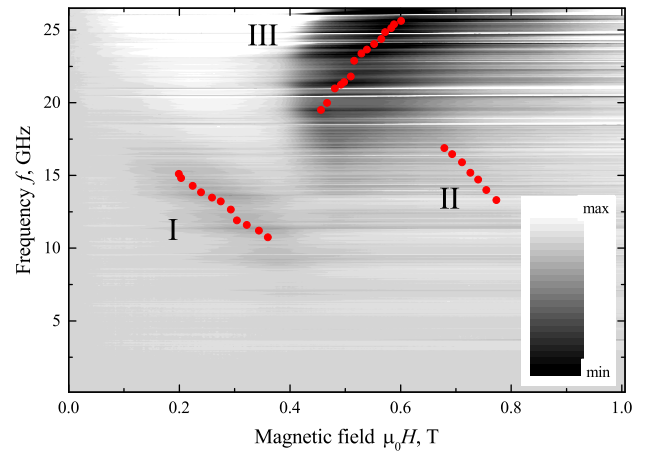


FIG. 4. FMR absorption spectra  $S_{21}(f, H)$  of  $\text{EuFe}_2\text{As}_2$  measured at  $T = 13$  K. Magnetic field is applied in-plane along  $ab$  crystal planes. Red dots highlight resonances attributed to the absorption features.

the magnetic field. Alternatively, the spectral feature III may be a trace of the acoustic mode of the domain with  $\phi_H = 0$  and  $H > H_a^{sat}$ . The origin of the spectral feature III can be verified by studying temperature dependence of the spectrum. Figure 4 shows FMR absorption spectrum of  $\text{EuFe}_2\text{As}_2$  sample measured at magnetic field applied in-plane along  $ab$  layers at  $T = 13$  K. The spectrum contains the same three absorption features (highlighted with red dots). The resonance line I at  $0.2 < \mu_0 H \lesssim 0.4$  T and  $10 < f < 15$  GHz corresponds to resonance of Eu spins aligned against the external field in the domain having the angle  $\phi_H = 0$  with the external field. A weak resonance line II at  $0.7 \lesssim \mu_0 H \lesssim 0.8$  T and  $12 < f < 18$  GHz corresponds to the optical antiferromagnetic response in the domain having the angle  $\phi_H = \pi/2$  with the external field. The spectral feature III at  $T = 5$  K (Fig. 2a) is transformed at  $T = 13$  K into a clearly distinguishable resonance line at  $\gtrsim 0.45\mu_0 H \gtrsim 0.7$  T and  $18 < f < 26$  GHz, thus, manifesting the acoustic mode of the domain with  $\phi_H = 0$  and  $H > H_a^{sat}$ . Lines I and III indicate that the spin-flip field at  $T = 13$  K is reduced to  $H_a^{sat} \approx 0.4$  T.

The overall correspondence between experimental and theoretical lines in Fig. 3 and established nature of all lines in Figs. 3 and 4 confirm validity of the free energy relation in Eq. 1 with the anisotropic Eu-Eu exchange interaction and bi-quadratic Eu-Fe exchange interaction for  $\text{EuFe}_2\text{As}_2$  compound together with the domain twinning concept of its orthorhombic crystal structure.

#### IV. CONCLUSION

In conclusion, in this work we report ferromagnetic resonance spectroscopy of  $\text{EuFe}_2\text{As}_2$  single crystals. The spectrum reveals several resonance features attributed

to antiferromagnetic resonances of Eu sub-lattice. By employing the recently proposed spin Hamiltonian with anisotropic Eu-Eu exchange interaction and bi-quadratic Eu-Fe exchange interaction, the spectral features have been attributed to antiferromagnetic and collective resonances of Eu layers in orthorhombic twinned crystal with different orientation of twin domains with respect to the external field. The obtained magnetic parameters are consistent with those reported previously, thus, confirming the complex biquadratic Hamiltonian for Eu spins in

EuFe<sub>2</sub>As<sub>2</sub> proposed earlier.

## V. ACKNOWLEDGMENTS

This work was supported by the Russian Science Foundation and by the Ministry of Science and Higher Education of the Russian Federation.

- 
- [1] Z. Ren, Z. Zhu, S. Jiang, X. Xu, Q. Tao, C. Wang, C. Feng, G. Cao, and Z. Xu, *Phys. Rev. B* **78**, 052501 (2008).
- [2] H. S. Jeevan, Z. Hossain, D. Kasinathan, H. Rosner, C. Geibel, and P. Gegenwart, *Phys. Rev. B* **78**, 052502 (2008).
- [3] S. Jiang, Y. Luo, Z. Ren, Z. Zhu, C. Wang, X. Xu, Q. Tao, G. Cao, and Z. Xu, *New J. Phys.* **11**, 025007 (2009).
- [4] Y. Xiao, Y. Su, M. Meven, R. Mittal, C. M. N. Kumar, T. Chatterji, S. Price, J. Persson, N. Kumar, S. K. Dhar, et al., *Phys. Rev. B* **80**, 174424 (2009).
- [5] Y. Xiao, Y. Su, W. Schmidt, K. Schmalzl, C. M. N. Kumar, S. Price, T. Chatterji, R. Mittal, L. J. Chang, S. Nandi, et al., *Phys. Rev. B* **81**, 220406 (2010).
- [6] S. Zapf, C. Stingl, K. Post, J. Maiwald, N. Bach, I. Pietsch, D. Neubauer, A. Löhle, C. Clauss, S. Jiang, et al., *Phys. Rev. Lett.* **113**, 227001 (2014).
- [7] J. Maiwald, I. I. Mazin, and P. Gegenwart, *Phys. Rev. X* **8**, 011011 (2018).
- [8] J. J. Sanchez, G. Fabbris, Y. Choi, Y. Shi, P. Malinowski, S. Pandey, J. Liu, I. I. Mazin, J.-W. Kim, P. Ryan, et al., *Phys. Rev. B* **104**, 104413 (2021).
- [9] Z. Ren et al., *Phys. Rev. Lett.* **102**, 137002 (2009).
- [10] G. Cao, S. Xu, Z. Ren, S. Jiang, C. Feng, and Z. Xu, *Journal of Physics: Condensed Matter* **23**, 464204 (2011).
- [11] H. S. Jeevan et al., *Phys. Rev. B* **83**, 054511 (2011).
- [12] S. Nandi et al., *Phys. Rev. B* **89**, 014512 (2014).
- [13] V. S. Stolyarov et al., *Sci. Adv.* **4**, eaat1061 (2018).
- [14] S. Grebenchuk et al., *Phys. Rev. B* **102**, 144501 (2020).
- [15] Y. Liu, Y.-B. Liu, Z.-T. Tang, H. Jiang, Z.-C. Wang, A. Ablimit, W.-H. Jiao, Q. Tao, C.-M. Feng, Z.-A. Xu, et al., *Phys. Rev. B* **93**, 214503 (2016).
- [16] Y. Liu, Y.-B. Liu, Y.-L. Yu, Q. Tao, C.-M. Feng, and G.-H. Cao, *Phys. Rev. B* **96**, 224510 (2017).
- [17] M. P. Smylie, K. Willa, J.-K. Bao, K. Ryan, Z. Islam, H. Claus, Y. Simsek, Z. Diao, A. Rydh, A. E. Koshelev, et al., *Phys. Rev. B* **98**, 014503 (2018).
- [18] T. K. Kim, K. S. Pervakov, D. V. Evtushinsky, S. W. Jung, G. Poelchen, K. Kummer, V. A. Vlasenko, A. V. Sadakov, A. S. Usoltsev, V. M. Pudalov, et al., *Phys. Rev. B* **103**, 174517 (2021).
- [19] T. Kim, K. Pervakov, V. Vlasenko, A. Sadakov, A. Usoltsev, D. Evtushinsky, S. Jung, G. Poelchen, K. Kummer, D. Roditchev, et al., *Phys. Usp.* (2021).
- [20] K. Iida, Y. Nagai, S. Ishida, M. Ishikado, N. Murai, A. D. Christianson, H. Yoshida, Y. Inamura, H. Nakamura, A. Nakao, et al., *Phys. Rev. B* **100**, 014506 (2019).
- [21] S. Ishida, D. Kagerbauer, S. Holleis, K. Iida, K. Munakata, A. Nakao, A. Iyo, H. Ogino, K. Kawashima, M. Eisterer, et al., *PNAS* **118**, e2101101118 (2021).
- [22] A. N. Bogdanov, A. V. Zhuravlev, and U. K. Rößler, *Phys. Rev. B* **103**, 174517 (2021).
- [23] S. M. Rezende, A. Azevedo, and R. L. Rodríguez-Suárez, *J. Appl. Phys.* **126**, 151101 (2019).
- [24] I. Golovchanskiy and V. Stolyarov, *J. Appl. Phys.* **submitted** (2021).
- [25] K. S. Pervakov, V. A. Vlasenko, E. P. Khlybov, A. Zaleski, V. M. Pudalov, and Y. F. Eltsev, *Supercond. Sci. Technol.* **26**, 015008 (2013).
- [26] V. Vlasenko, K. Pervakov, and S. Gavrilkin, *Supercond. Sci. Technol.* **33**, 084009 (2020).
- [27] I. Neudecker, G. Woltersdorf, B. Heinrich, T. Okuno, G. Gubbiotti, and C.H.Back, *J. Mag. Mag. Mater.* **307**, 148 (2006).
- [28] S. S. Kalarickal, P. Krivosik, M. Wu, C. E. Patton, M. L. Schneider, P. Kabos, T. J. Silva, and J. P. Nibarger, *J. Appl. Phys.* **99**, 093909 (2006).
- [29] D. MacNeill, J. T. Hou, D. R. Klein, P. Zhang, P. Jarillo-Herrero, and L. Liu, *Phys. Rev. Lett.* **123**, 047204 (2021).
- [30] H. Suhl, *Phys. Rev.* **97**, 555 (1955).
- [31] J. Smit and H. G. Beljers, *Philips Res. Rep.* **10**, 113 (1955).
- [32] Z. Zhang, L. Zhou, P. E. Wigen, and K. Ounadjela, *Phys. Rev. B* **50**, 6094 (1994).
- [33] D. S. Schmooly and J. M. Barandiaran, *J. Phys.: Condens. Matter* **10**, 10679 (1998).
- [34] J. Lindner and K. Baberschke, *J. Phys.: Condens. Matter* **15**, S465 (2003).